Environmental Research Letters

LETTER

Analysing the origin of rain- and subsurface water in seasonal wetlands of north-central Namibia

Tetsuya Hiyama[1,8], Hironari Kanamori[1], Jack R Kambatuku[2], Ayumi Kotani[3], Kazuyoshi Asai[4], Hiroki Mizuochi[5], Yuichiro Fujioka[6] and Morio Iijima[7]

[1] Institute for Space-Earth Environmental Research, Nagoya University, Nagoya, Japan
[2] Faculty of Agriculture and Natural Resources, University of Namibia, Oshakati, Namibia
[3] Graduate School of Bioagricultural Sciences, Nagoya University, Nagoya, Japan
[4] Geo-Science Laboratory Co. Ltd, Nagoya, Japan
[5] Graduate School of Life and Environmental Sciences, University of Tsukuba, Tsukuba, Japan
[6] Frontier Research Institute for Interdisciplinary Sciences, Tohoku University, Sendai, Japan
[7] Faculty of Agriculture, Kindai University, Nara, Japan
[8] Author to whom any correspondence should be addressed.

E-mail: hiyama@nagoya-u.jp

OPEN ACCESS

RECEIVED
20 September 2016

REVISED
20 December 2016

ACCEPTED FOR PUBLICATION
24 January 2017

PUBLISHED
2 March 2017

Keywords: stable water isotopes (SWIs), rainwater, surface water, subsurface water, atmospheric water budget, recycled water, evaporation of raindrops

Supplementary material for this article is available online

Abstract

We investigated the origins of rain- and subsurface waters of north-central Namibia's seasonal wetlands, which are critical to the region's water and food security. The region includes the southern part of the Cuvelai system seasonal wetlands (CSSWs) of the Cuvelai Basin, a transboundary river basin covering southern Angola and northern Namibia. We analysed stable water isotopes (SWIs) of hydrogen (HDO) and oxygen ($H_2{}^{18}O$) in rainwater, surface water and shallow groundwater. Rainwater samples were collected during every rainfall event of the rainy season from October 2013 to April 2014. The isotopic ratios of HDO (δD) and oxygen $H_2{}^{18}O$ ($\delta^{18}O$) were analysed in each rainwater sample and then used to derive the annual mean value of (δD, $\delta^{18}O$) in precipitation weighted by each rainfall volume. Using delta diagrams (plotting δD vs. $\delta^{18}O$), we showed that the annual mean value was a good indicator for determining the origins of subsurface waters in the CSSWs. To confirm the origins of rainwater and to explain the variations in isotopic ratios, we conducted atmospheric water budget analysis using Tropical Rainfall Measuring Mission (TRMM) multi-satellite precipitation analysis (TMPA) data and ERA-Interim atmospheric reanalysis data. The results showed that around three-fourths of rainwater was derived from recycled water at local–regional scales. Satellite-observed outgoing longwave radiation (OLR) and complementary satellite data from MODerate-resolution Imaging Spectroradiometer (MODIS) and Advanced Microwave Scanning Radiometer (AMSR) series implied that the isotopic ratios in rainwater were affected by evaporation of raindrops falling from convective clouds. Consequently, integrated SWI analysis of rain-, surface and subsurface waters, together with the atmospheric water budget analysis, revealed that shallow groundwater of small wetlands in this region was very likely to be recharged from surface waters originating from local rainfall, which was temporarily pooled in small wetlands. This was also supported by tritium (^3H) counting of the current rain- and subsurface waters in the region. We highly recommend that shallow groundwater not be pumped intensively to conserve surface and subsurface waters, both of which are important water resources in the region.

1. Introduction

Wetlands cover 6% of the Earth's land surface and have great hydrological and ecological significance. Agricultural use of wetlands is important for food security (Hiyama *et al* 2014). However, land-use changes in wetland areas can alter the water budget and ecosystem. To conserve these environments, great

care is needed when introducing new cropping systems. In particular, land-use changes in wetlands alter evapotranspiration, a major component of the water budget, which can affect the water cycle and ecosystems (Suzuki *et al* 2014).

Namibia, located in southern Africa, has an area of 824 000 km^2, a population of about 2 364 000 people, and a gross national income (GNI) of 4510 USD per capita (The World Bank 2012). With its rich mineral resources, Namibia's economy grew by 4.8% from 2009 to 2010 (The World Bank 2012). However, Namibia is one of the least equitable countries in the world, as shown by a Gini index of 64–74 (United Nations Development Programme 2007, The World Bank 2012). Approximately 40% of the population lives in north-central Namibia (Mendelsohn *et al* 2013), where most residents are subsistence farmers cropping pearl millet *Pennisetum glaucum* as a staple food, as well as raising livestock. Food production in the region has been unstable due to large inter-annual variations in precipitation, highlighting its lack of food security.

North-central Namibia is characterised by a semi-arid climate. The rainy season starts in the middle of November and ends in the middle of April of the following year. The dry season extends from mid-April to mid-November. In the rainy season, surface (flooding) water flows from the Angolan Plateau and creates a vast seasonal wetland. The region, locally called the Cuvelai system seasonal wetlands (CSSWs), occupies the southwestern part of the Cuvelai Basin (Mendelsohn *et al* 2013, Njunge 2013). The amount of surface water has varied widely in the last 10 year, causing either serious deluge or drought in the region. The water resources of the CSSWs are largely used for grazing and fishing rather than for cropping. The limited use of these water resources is due to the unstable flood intensity and because the Etosha Pan, the largest salt pan in Africa (figure 1), located at the southern edge of the Cuvelai Basin, is a national wildlife sanctuary. If large-scale agricultural development were to occur in this region, the vulnerable wetland environment may be harmed.

Since 2011, we have been conducting research aimed at developing a flood- and drought-adaptive cropping system (FDACS) that can preserve water environments and cope with yearly fluctuations in rainfall. The FDACS was developed through trials in the fields of crop science, development studies, hydrology, and integrated studies (Hiyama *et al* 2014). This paper focuses on the hydrological aspects and provides information for evaluating water budgets if a rice-based, mixed-cropping system (as one of the schemes of FDACS) were introduced to the region. There have been several large-scale projects that transformed vast areas of wetlands to agricultural fields in the region (Iijima *et al* 2013). The pumping of shallow groundwater has also been attempted in other regions of northern Namibia. to supply water resources for agricultural use in the wetlands. However, the purpose of our project is to introduce a rice-based, mixed-cropping system to small wetlands, which are individually owned by local subsistence farmers and/or residents, while supporting the conservation of water environments in small wetlands.

Recently, Mizuochi *et al* (2014) detected the distribution of surface water with high spatial and temporal resolution by using two types of complementary satellite data—MODerate-resolution Imaging Spectroradiometer (MODIS) and Advanced Microwave Scanning Radiometer–Earth Observing System (AMSR-E)—as well as AMSR2 after AMSR-E became unavailable. They then aggregated the extracted water presence maps into probability of water presence (PWP) maps for the rainy season and the whole year, and estimated the area potentially suitable for rice cultivation. The PWP maps revealed the total area potentially suitable for rice cultivation as 1 255 km^2 (1.6% of the total study area [78 440 km^2] within the CSSWs region). An area for the potential introduction of a rice–pearl millet mixed-cropping system is currently being estimated.

Although there are several publications focusing on the geographical, hydrological, and agricultural aspects of the region (Mendelsohn *et al* 2000, 2002, 2013, Christelis and Struckmeier 2001, IAEA 2007), studies on the origins of rain- and subsurface waters in small wetlands of the CSSWs remain insufficient. This study aims to evaluate the origins of rain- and subsurface waters in the basin. We analysed stable water isotopes (SWIs) of hydrogen (HDO) and oxygen ($H_2{}^{18}O$) in rainwater, surface water and subsurface water (or shallow groundwater). Tritium (^3H) counting was also conducted to support the SWI analyses. Additionally, the atmospheric water budget was analysed using atmospheric reanalysis data to confirm the origins of rainwater and the seasonal variability of convective activity, which is a good indicator of recycled water at local–regional scales.

2. Methods

2.1. Study site

Figure 1 shows river networks in southern Africa (figure 1(*a*)) and the topography of the Cuvelai Basin. The locations of main cities and the study site are indicated in figure 1(*b*). The Cuvelai Basin lies between the Kunene and Okavango rivers in Angola and Namibia. The northern edge of the basin is on the Angolan Plateau. The southern part of the basin is located in north-central Namibia, and the southern edge forms the Etosha Pan. The CSSW region has transboundary seasonal river networks (*iishana*) and small wetlands (*oomdombe*) formed during the rainy season at higher elevation between the river networks. The region has extremely flat topography with an average terrain slope of 1/3300. There are no

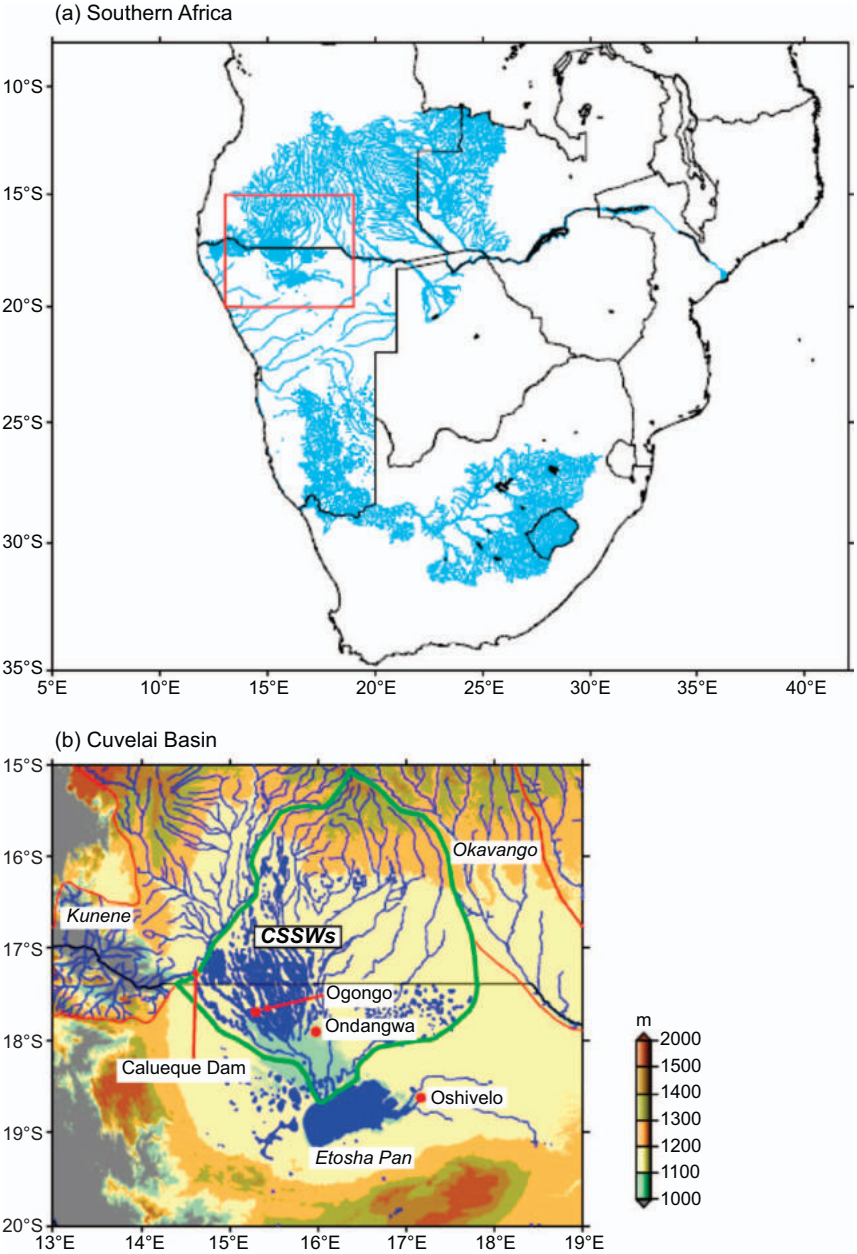

Figure 1. (*a*) Map of river networks in southern Africa. (*b*) The study area (red square) along with the topography and river networks in/around the Cuvelai Basin. The river networks were obtained from the 'Digital Atlas of Namibia' (www.uni-koeln.de/sfb389/e/e1/download/atlas_namibia/main_namibia_atlas.html), which was based on the Atlas of Namibia Project (2002), Ministry of Environment and Tourism (Mendelsohn *et al* 2002). Digital elevation data shown in (*b*) was based on SRTM 90 m Digital Elevation Database v4.1 (www.cgiar-csi.org/data/srtm-90m-digital-elevation-database-v4-1).

permanent rivers except the transboundary Kunene river (Christelis and Struckmeier 2001). The *iishana* converge at the Omadhiya Lakes and then flow into the Etosha Pan (Mendelsohn *et al* 2013).

The mean annual rainfall in the Cuvelai Basin is about 400 mm. There is an east–west rainfall gradient across the Cuvelai Basin as a result of moist air feeding in from the north and northeast during the rainy season. Because of this, the southwestern parts of the basin receive on average only around 250 mm per annum, while the northeast receives about 600 mm (Mendelsohn *et al* 2013).

The Ogongo campus of the University of Namibia (UNAM) was the main research site of this study (figure 1(*b*)). The campus is located on the south-central part of the CSSW region. Around the campus, there are dense–sparse mopane (locally called the *omusati* tree) communities. The water of a small wetland (*ondombe*) or wetlands (*oomdombe*) in the CSSWs, formed during the rainy season, is a critical resource for domestic, livestock and food production. There is a reservoir (Calueque Dam; Mendelsohn *et al* 2000) of the Kunene river around 100 km northwest from the Ogongo campus that supplies water resource to cities and towns in north-central Namibia. A canal originating from the Calueque Dam of the Kunene river flows along 'Road C46'.

2.2. Isotope analyses and water sampling

The stable water isotopologues HDO and $H_2{}^{18}O$, referred to as SWIs, are plausible hydroclimate proxy candidates. The concentrations of SWIs are expressed in δ notation: δD or $\delta^{18}O = (R_{sample}/R_{V\text{-}SMOW} - 1) \times 1\,000$, where R is the isotopic ratio (HDO/H_2O or $H_2{}^{18}O/H_2{}^{16}O$) [‰], and V-SMOW is Vienna Standard Mean Ocean Water. To understand the water sources of small wetlands in the CSSW region, SWIs in rain-, surface, and subsurface waters were analysed. The analyses of δD and $\delta^{18}O$ were conducted using a liquid water isotope analyser (LGR model DLT-100; Los Gatos Research Inc., Mountain View, CA, USA). The accuracy of the analyses was ±0.5‰ for δD and ±0.1‰ for $\delta^{18}O$. The analyses of δD and $\delta^{18}O$ were conducted at the Geo-Science Laboratory Co. Ltd, Nagoya, Japan.

The ^3H concentration of precipitation peaked around 1963 due to nuclear testing, and the half-life of ^3H is relatively short. Therefore, if the mean residence time of subsurface water is around 50–60 years, the ^3H concentrations of the water could be a useful tracer to detect the extent to which the subsurface water originated from precipitation after nuclear testing. To determine the residence time of subsurface water in the region, ^3H counting was conducted using a low-background liquid scintillation counter (Model LB-5; Hitachi-Aloka, Tokyo, Japan) following electrolytic enrichment of ^3H by a factor of about 25 using Fe–Ni electrodes (see also Hiyama *et al* 2013). The total analytical precision was better than 0.23 tritium units (TU). The ^3H measurements were also conducted at the Geo-Science Laboratory Co. Ltd, Nagoya, Japan.

The water samples were taken around Ogongo campus. A preliminary rainwater sample was taken at Onembamba village, Omusati region (17° 25′ 09.11″ S, 15° 13′ 37.77″ E) on 27 December 2012, as well as at the Ogongo campus (17° 40′ 35.20″ S, 15° 17′ 31.53″ E) on 11 March 2013. The rainfall in both cases was relatively intense and supposedly from convective clouds. A 2 L plastic container attached with a funnel was used to collect rainwater samples. To prevent direct evaporation from the collected rainwater, a ping-pong ball was placed in the funnel. Rainwater samples were removed from the container about 3 h after rainfall had stopped.

Intensive rainwater sampling campaigns were done at the Ogongo campus in the 2013–2014 rainy season. Samples from every rainfall event in the rainy season, from 16 October 2013 to 22 April 2014, were taken. These water samples were used to evaluate annual mean values of rainwater SWIs in the region.

Surface water from a small wetland near the Ogongo campus (17° 40′ 48.14″ S, 15° 18′ 59.14″ E) was taken on 11 March 2013. This surface water was the water remaining after a rainfall event on 10–11 March 2013. Subsurface water from 2.9 m below the ground surface was taken at Onembamba village, Omusati region (17° 25′ 17.45″ S, 15° 13′ 41.07″ E) on 18 December 2012, and at the Ogongo campus on 8 and 9 May 2013. Additionally, canal water flowing along Road C46 and irrigation water at the experimental sloped field of the Ogongo campus, both originating from the Kunene river, were sampled at the beginning of March 2013.

2.3. Atmospheric water budget analyses

Satellite-based measurement data and atmospheric reanalysis data were used to analyse the atmospheric water budget. To evaluate regional rainfall amounts in the Cuvelai Basin, Tropical Rainfall Measuring Mission (TRMM) multi-satellite precipitation analysis (TMPA) 3B42 version 7 data (Huffman *et al* 2007) were used. This dataset is created by blending passive microwave data collected by the TRMM Microwave Imager (TMI), Special Sensor Microwave Imager (SSM/I), AMSR-E, Advanced Microwave Sounding Unit B (AMSU-B), and infrared (IR) data acquired by the international constellation of geosynchronous Earth orbit (GEO) satellites, and based on calibration by the precipitation estimates of the TMI precipitation radar (TMI-PR) combined algorithm (Kanamori *et al* 2013). This dataset covers both temporally and spatially consecutive data from 50° S to 50° N every 3 h, with a horizontal resolution of 0.25° × 0.25°. Daily precipitation [mm d^{-1}] was calculated using the 3 h ourly original data in this study.

We also used the ERA-Interim atmospheric reanalysis data (Dee *et al* 2011); the horizontal resolution was 0.75° × 0.75°. Precipitable water [mm] and atmospheric moisture fluxes in qu (zonal component) and qv (meridional component) [kg m^{-1} s^{-1}] were used in this study. The precipitable water and atmospheric moisture fluxes were vertically integrated from the bottom to the top of the atmosphere in the reanalysis model field. The data were calculated from 6 h (00, 06, 12, and 18 UTC) to daily original data.

The concept of atmospheric water budget analysis (Peixoto and Oort 1983, 1992) was applied using the following equations:

$$\frac{\partial PW}{\partial t} = -\nabla\cdot\frac{1}{g}\int_{P_b}^{P_t} q\boldsymbol{v}\mathrm{d}p + E - P = -\nabla\cdot\langle q\boldsymbol{v}\rangle + E - P \quad (1)$$

$$E = P - C + Q \quad (2)$$

where, E is evapotranspiration, P is precipitation, C is the atmospheric moisture flux convergence and Q is the temporal change in the precipitable water PW, which is an integral of q in the atmospheric column. The terms g, q and $\boldsymbol{v}$ represent acceleration due to gravity, specific humidity and the horizontal wind vector, respectively. The integral in the first term on the right-hand side of equation (1) and PW range from the bottom (P_b) to the top of the atmosphere (P_t).

We evaluated each component of equation (2) from 1 September 2013 to 31 May 2014. For the atmospheric water budget evaluation, P was obtained

from the TRMM 3B42 data, C and Q were calculated using ERA-Interim reanalysis data and E was evaluated as the residual of equation (2). We used TRMM precipitation instead of ERA-Interim precipitation mainly because the latter does not assimilate observed precipitation data directly, but also because the data are projected (modelled) using atmospheric variables.

To compare the atmospheric water budget (especially the recycled water in CSSWs) with the isotopic ratio of rainwater, the local water recycling ratio (LWRR) was defined with the following equations.

$$\begin{aligned} \mathrm{LWRR} &= (P - C + Q)/P \times 100[\%] \\ &= E/P \times 100[\%] \end{aligned} \quad (3)$$

The LWRR primarily ranged between 0 and 100; it should be 0 when $E = 0$ and 100 when $E = P$.

2.4. Other data sources

The Outgoing Longwave Radiation–Daily Climate Data Record (OLR-Daily CDR) (Lee 2014, Lee *et al* 2014) was used as a proxy for convective activities over the region (17–18° S, 15–16° E). The OLR-Daily CDR, with a resolution of 1° × 1°, was derived using the radiance observations from the High-resolution Infrared Radiation Sounder (HIRS) on board the NOAA TIROS-N series and the Eumetsat MetOp-A satellites.

Additionally, two types of complementary satellite data from the MODIS and AMSR series (AMSR-E and AMSR2) were used. The data were analysed to estimate the ratio of surface water coverage. We combined the modified normalised difference water index (MNDWI) (Xu 2006) from the MODIS data with the normalised difference polarisation index (NDPI) from the AMSR-E and AMSR2 data. The area of surface water was determined based on a gap-filling method (database unmixing) with the above-mentioned two indices, providing daily 500 m-resolution MNDWI maps in the region (17–18° S, 15–16° E) regardless of whether the sky was clear (Mizuochi *et al* 2014). Finally, the daily value of the surface water coverage ratio (SWCR) was extracted.

During the study period, surface meteorological data were collected using the Bowen ratio measuring system (C-AWS-BW3, Climatec, Japan) on Ogongo Campus. Air temperature and relative humidity were measured at a height of 3.0 m by a ventilated sensor (HMP-155D, Vaisala, Finland), and a tipping bucket rainfall gauge (RT-5 E, Ikeda-keiki, Japan) was used in this study.

3. Results

3.1. Stable water isotopes (SWIs) and tritium (^{3}H)

A total of 41 rainfall events were observed during the rainy season from 16 October 2013 to 22 April 2014. The total observed rainfall at the Ogongo campus of UNAM was 479.5 mm. There were several dry spells in December 2013, as well as in January 2014 and February 2014. The analysed isotopic ratios (δD and δ^{18}O) were very high at the beginning of the rainy season (October and November) and the value was relatively high during low rainfall intensity (figure 2). However, there were a few high-intensity rainfall events with high isotopic ratios (1–2 of December 2013 and 21–22 of January 2014). In the former, abrupt decreases in the isotopic ratios were observed, whereas the latter case occurred after a sudden increase in isotopic ratios. These drastic changes in isotopic ratios corresponded to evaporation processes, which will be described later.

The δD and δ^{18}O from each rainfall event were used to obtain annual mean values of δD and δ^{18}O, both of which were weighted by the amount rainfall in each event. Before this calculation, we excluded isotopic values from events with <30 cm^3 rainfall to avoid any results skewed by artificial or unexpected evaporation in small sample volumes. The total volume of the rainwater samples used for the calculations was 6774.5 cm^3 (89% of a total 7 615.5 cm^3). Finally, the annual mean values of δD and δ^{18}O, weighted by each rainfall amount, were calculated as (δ^{18}O, δD) = (−7.4, −47.2) from 29 rainfall samples (shown as weighted mean value [WMV] in figure 3). This was relatively low compared with the value reported in the literature of (δ^{18}O, δD) = (−5.9, −37.7) (IAEA 2007), which was from precipitation samples collected in the central part of the Oshivelo artesian aquifer region (Christelis and Struckmeier 2001), about 300 km southeast of the Ogongo campus. This difference may be due to the precipitation system or the origin of the water vapour.

The δD and δ^{18}O in rainwater overlay the global meteoric water line (GMWL), an equation defined by Craig (1961) as the average relationship between δD and δ^{18}O in natural terrestrial waters (figure 3). However, the relationships between δD and δ^{18}O in surface and subsurface waters (shallow groundwater) diverge from the GMWL (figure 4) and represent different equations with slopes of 5 ($\delta D = 5 \times \delta^{18}O - 10.2$) or < 5. This indicates that both surface and subsurface waters were affected by direct evaporation of raindrops and pooled surface water in the small wetlands. Because the sampled subsurface water was shallow groundwater following strong rainfall, it is very likely to be recharged from the pooled surface waters of wetlands after rainfall events.

This was also supported by the ^{3}H counting. The mean ^{3}H value of the shallow groundwater sampled at Onembamba village on 18 December 2012 was 3.6 ± 0.1 (0.43 ± 0.02 Bq L^{-1}). ^{3}H values of rainwater sampled at the same village (27 December 2012) and the Ogongo campus (11 March 2013) were 3.1 ± 0.1 (0.37 ± 0.02 Bq L^{-1}) and 3.3 ± 0.1 (0.39 ± 0.02 Bq L^{-1}), respectively. This indicates that the bulk age of the shallow

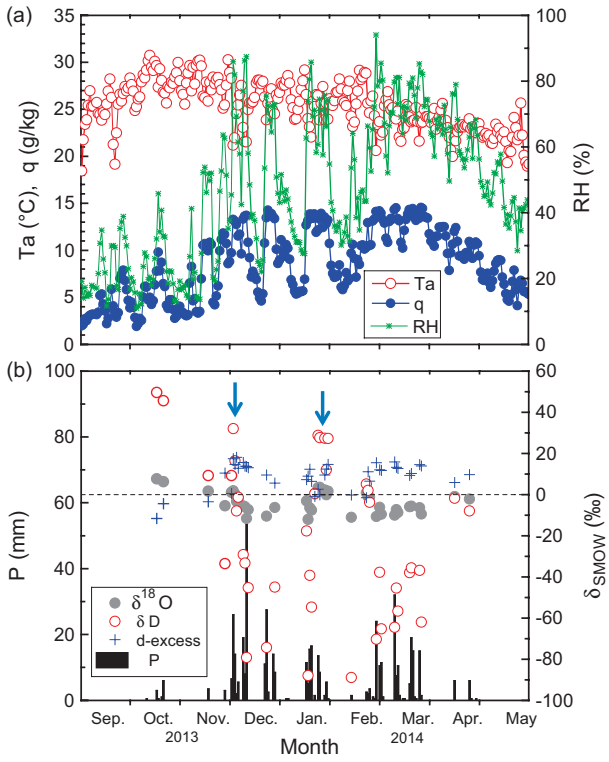

Figure 2. Time series of (*a*) air temperature (*Ta*; °C), relative humidity (*RH*; %), specific humidity (*q*; g kg^{-1}), (*b*) stable isotopic ratio of deuterium (*δ*D; ‰), oxygen-18 (δ^{18}O; ‰), deuterium-excess (d-excess; ‰; defined as d-excess = $\delta D - 8 \times \delta^{18}O$), and daily rainfall (*P*; mm d^{-1}) from 1 September 2013 to 31 May 2014, observed at Ogongo campus of the University of Namibia. Arrows indicate the rainfall events from 1–2 December 2013 and 21–22 January 2014.

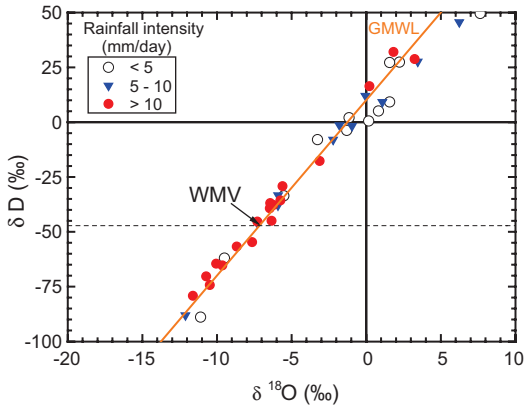

Figure 3. Delta diagram showing the isotopic ratio of HDO (*δ*D) and $H_2{}^{18}O$ (δ^{18}O) in rainwater obtained from 16 October 2013 to 22 April 2014. The straight line is the global meteoric water line (GMWL), $\delta D = 8 \times \delta^{18}O + 10$ (see Craig 1961). The weighted mean values (WMVs) of *δ*D and δ^{18}O were (δ^{18}O, *δ*D) = (−7.4, −47.2) based on 29 rainfall samples.

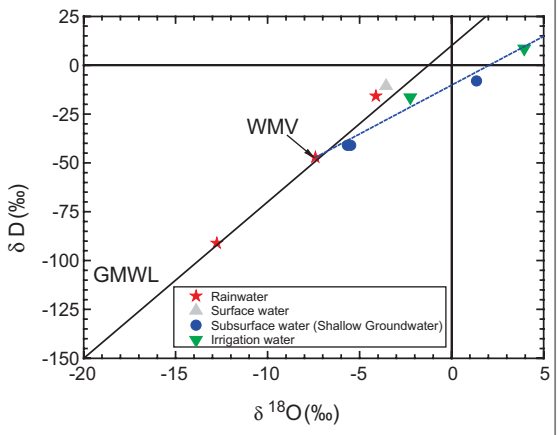

Figure 4. Delta diagram showing the *δ*D and δ^{18}O in rainwater, surface water and subsurface water (shallow groundwater) in the study area. The two rainwater samples were taken at Onembamba village of Omusati region (17° 25′ 09.11″ S, 15° 13′ 37.77″ E) on 27 December 2012 and at the Ogongo campus of UNAM (17° 40′ 35.20″ S, 15° 17′ 31.53″ E) on 11 March 2013. Also plotted were the canal and irrigation water, which came from the Calueque Dam of the Kunene river (see figure 1). The WMVs of *δ*D and δ^{18} were (δ^{18}O, *δ*D) = (−7.4, −47.2) based on 29 rainfall samples from 16 October 2013 to 22 April 2014 (see figure 3). The dashed straight line indicates $\delta D = 5 \times \delta^{18}O - 10.2$. GMWL is also shown.

groundwater was young and thus it was not old groundwater flowing from an upstream aquifer. For reference, ^{3}H values from water used for irrigation at the experimental sloped field on the Ogongo campus, and water from a canal flowing along Road C46, were 3.0 ± 0.1 (0.35 ± 0.02 Bq L^{-1}) and 2.8 ± 0.1 (0.34 ± 0.02 Bq L^{-1}), respectively. Because both originated from the Kunene River basin and its main reservoir (Calueque Dam), the residence times of the canal and irrigation water were almost the same as, or slightly different from, the subsurface water (shallow groundwater) sampled at/around Ogongo.

3.2. Atmospheric water budget

To confirm the origins of rainwater and to explain the variations of the isotopic ratios, we conducted

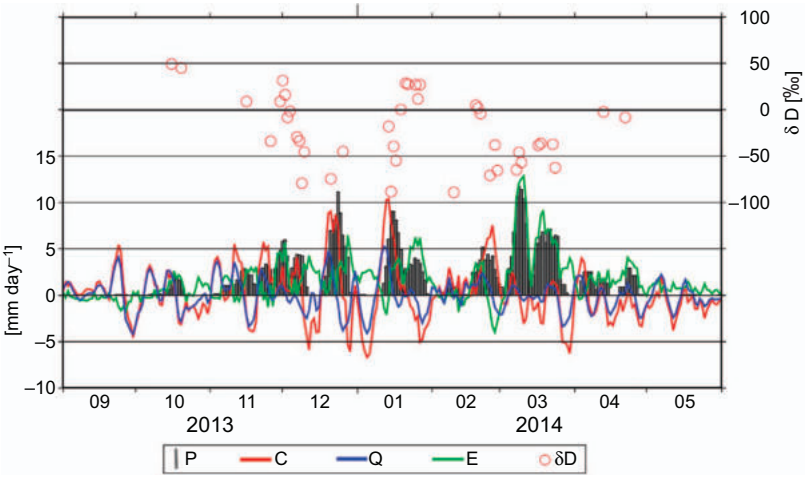

Figure 5. Time series of 5 d running average atmospheric water budget components from 1 September 2013 to 31 May 2014 at and around the CSSW region (17–18° S, 15–16° E). P is precipitation [mm d^{-1}], C is atmospheric moisture flux convergence [mm d^{-1}], Q is temporal change in precipitable water [mm d^{-1}], and E is evapotranspiration [mm d^{-1}]. P was obtained from TRMM 3B42, and C and Q were calculated using the ERA-Interim atmospheric reanalysis data based on equation (1). The value of E was the residual term of the atmospheric water budget, which was calculated from equation (2). The isotopic ratio of δD is also plotted.

atmospheric water budget analysis using TRMM 3B42 version 7 data and ERA-Interim atmospheric reanalysis data. Figure 5 shows time series of atmospheric water budget components from 1 September 2013 to 31 May 2014 at the CSSWs (17–18° S, 15–16° E). Precipitation (P), atmospheric moisture flux convergence (C), change in the precipitable water (Q), and evapotranspiration (E) were 5 d running average values. Temporal variations of C and Q corresponded very well before the start of the rainy season (before mid-October) as well as after (after mid-April). During the dry season, the variation of E was very small. After the rainy season began, during rainfall events, C increased first, followed by E as soon as C decreased. These features disappeared after around January (middle of the rainy season), and clear discrepancies among rainfall events (large C or E) were observed.

Interestingly, in the first half of the rainy season, rainwater obtained during large E events (i.e. in the latter half of each rainfall event) had high δD and δ^{18}O values, which implied that evaporation from the land surface dominated the latter half of each rainfall event at the beginning of the rainy season. It is also interesting that the contribution of E to P was very large (around 100%) during the two large rainfall events in March. Because the isotopic ratios of these two rainfall events were low, recycled water (i.e. contribution of E to P) could play an important role in these rainfall events.

Although temporal variations in the contributions of E and/or C to P were different among rainfall events, the overall contribution of E to P (namely LWRR) was large during the rainy season. The mean value of LWRR was 75% (when $P > 1$ mm d^{-1}), and thus around three-fourths of rainwater was derived from recycled water in the region. The value was relatively small at the beginning of the rainy season and large at the end (figure 5).

The LWRR time series mainly depended on seasonal variations in the conditions of the surface water coverage (or SWCR). Figure 6 shows time series of daily P, daily OLR, the isotopic ratio of δD, and the daily SWCR from 1 September 2013 to 31 May 2014. The target region is the same as in figure 5. It should be noted that OLR values at the beginning of the rainy season (from mid-October to early December) as well as at the end (April) were higher than those in the middle of the season. This means that cloud-top heights of the convective clouds were lower at the beginning and the end of the rainy season compared with those in the middle of the season.

In the middle of the rainy season, despite the low OLR values (i.e. high convective activity and therefore high cloud-top height), high isotopic ratios were observed in the rainwater. In these cases, SWCR values were low and thus almost all of the rainwater could evaporate immediately after falling to the ground surface. This means that equilibrium isotopic fractionation (Merlivat and Jouzel 1979) may not occur readily because of direct evaporation on the land surface. Simultaneously, evaporation of raindrops under the cloud-base height (i.e. in the atmospheric boundary layer, ABL) may occur readily during these events. The evaporation of raindrops falling through the dry ABL may produce high isotopic ratios in rainwater (by means of non-equilibrium fractionation).

Towards the end of the rainy season (in March), despite high OLR values (i.e. in low convective activities), the isotopic ratios were low. In these cases, both SWCR and LWRR values were high. This means that evaporated surface water could be recycled rainwater on relatively short time scales with adequate isotopic fractionation on the ground surface. Although just one year's data were used in this study, it should be mentioned that SWCR values were always

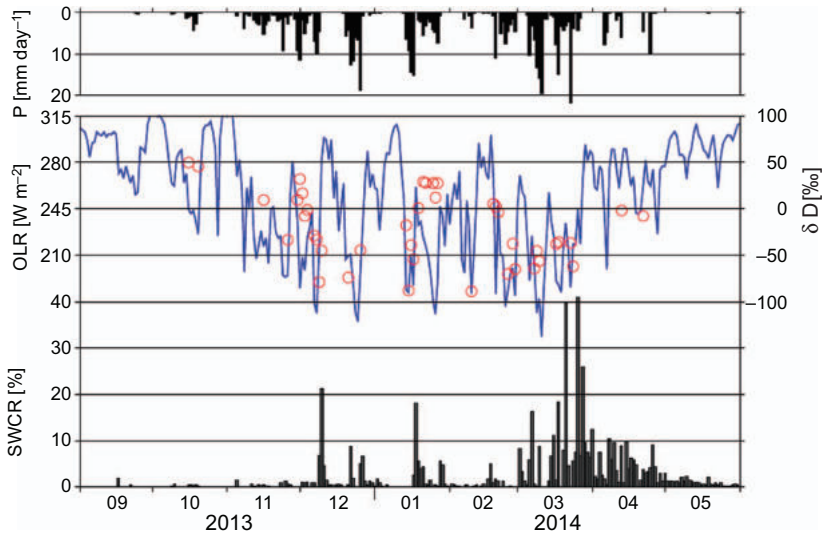

Figure 6. Time series of daily precipitation P [mm d^{-1}], satellite-based outgoing longwave radiation (OLR) [W m^{-2}], the isotopic ratio δD in rainwater obtained at Ogongo, and the surface water coverage ratio (SWCR) [%] from 1 September 2013 to 31 May 2014. The area is the same as in figure 5.

large at the end of the rainy season every year. Due to the surface water conditions, the effects of interannual variability of precipitation on LWRR were small, at least at the end of the rainy season (figure not shown).

4. Discussion

We found unique temporal variations in daily P, OLR, SWCR, LWRR, and δD. There were two large rainfall events in March with relatively high LWRR. Interestingly, the δD and δ^{18}O were low and the OLR was also very low (< 200 W m^{-2}) in both events (figures 5 and 6). Therefore, convective activities may be stronger than other events. Generally, δD and δ^{18}O decreased when the cloud-top heights of convective clouds were higher but the isotopic ratios increased when cloud-top heights were lower. Additionally, when the ABL was dry, isotopic ratios increased mainly because raindrop evaporation increased during descent from the cloud-base. This suggests that the two rainfall events with high LWRR in March were derived not only from stronger (higher cloud-top) convection, but also had relatively humid ABL conditions (figure 2(*a*)). Indeed, such wet atmospheric conditions in March were reasonable because the land surface was also wet enough (i.e. high SWCR) in the latter half of the rainy season (figure 6).

On the other hand, at the beginning of the rainy season or in drier atmospheric conditions, isotopic ratios in rainwater could be affected by a dry ABL. The isotopic values of rainwater samples in such conditions increased due to direct evaporation. It should be noted that isotopic ratios of rainwater collected from 1–2 December 2013 and from 21–22 January 2014 were high despite very intense rainfall (> 5 mm d^{-1}). In both cases, SWCR values were low (figure 6) and therefore it seems that both events were associated with immediate land surface evaporation with non-equilibrium fractionation or direct evaporation of raindrops below the cloud base.

The d-excess value, defined as d-excess $= \delta D - 8 \times \delta^{18}O$, is another useful value for tracking the origin of atmospheric moisture because it is relatively invariant during transport and during the formation of condensate accompanied by equilibrium isotopic fractionation (Kurita and Yamada 2008). Because non-equilibrium fractionation occurs during evaporation from the land surface, the d-excess of evaporated moisture exceeds that of surface water (Gat and Matsui 1991, Henderson-Sellers *et al* 2004). Therefore, large d-excess values may reflect the contribution of evaporation from the land surface to precipitation (Kurita and Yamada 2008). Although non-equilibrium fractionation during evaporation of falling raindrops has not been frequently reported, this study indicated that evaporation of falling raindrops results in high d-excess values in evaporated moisture and small d-excess values in residual raindrops. Interestingly, the d-excess values of the events in October and in November were very low (< 0; see figure 2). Therefore, direct evaporation of raindrops below the cloud base could be enhanced due to a dry ABL. On the other hand, the two cases (1–2 December and 21–22 January) may have experienced evaporation mainly on the land surface, because these d-excess values were relatively high. As described above, SWCR values were low in both cases, so almost all of the rainwater could evaporate immediately after falling down on to the ground surface.

Certainly, the isotopic ratios of rainwater may be affected by the water vapour origins, which can be revealed by synoptic conditions. Figure 7 shows the spatial pattern of vertically integrated moisture flux vectors and moisture flux convergence around

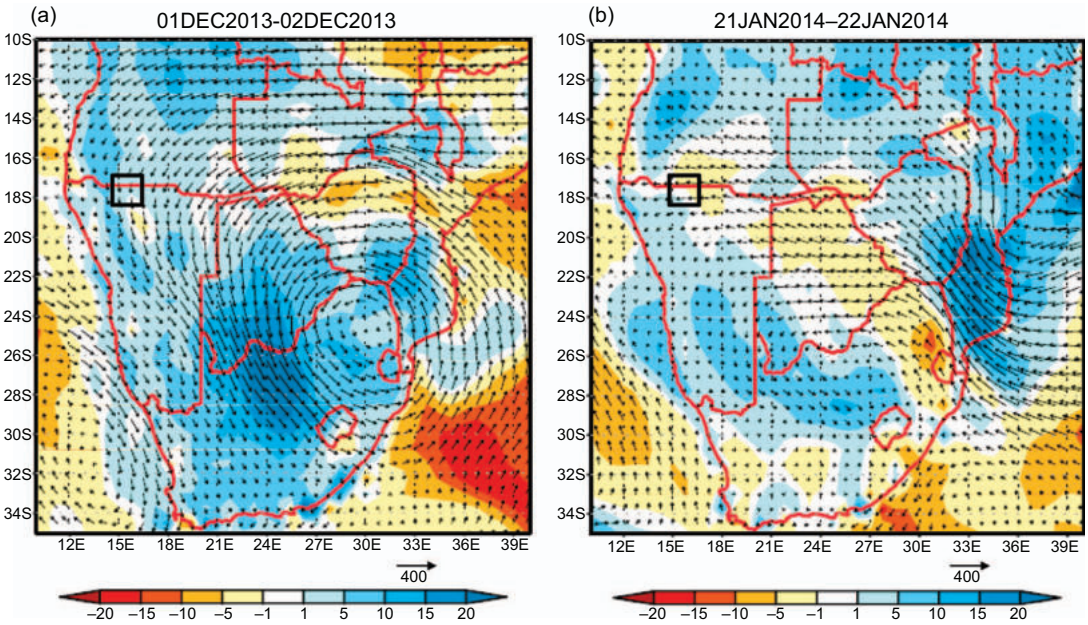

Figure 7. (*a*) Spatial pattern of vertically integrated moisture flux vectors (arrows; kg m^{-1} s^{-1}) and moisture flux convergence (colour shadings; mm d^{-1}) from 1–2 December 2013. Blue and red colours indicate convergence and divergence, respectively. (*b*) Same as (*a*) but for 21–22 January 2014.

southern Africa for both 1–2 December 2013 (figure 7(*a*)) and 21–22 January 2014 (figure 7(*b*)). In the former case, there were northerly moisture flux vectors from Angola to Namibia and moisture flux convergence was large in the CSSWs. In the latter case, there were easterly flux vectors along the border between Namibia and Angola, and moisture flux convergence did not appear in the region. Although the isotopic ratios of rainwater in both cases were high, synoptic moisture fields were quite different from each other. This means that the isotopic ratios of rainwater were not affected by the synoptic moisture fields, but rather were largely influenced by atmospheric processes, including direct evaporation of raindrops falling to the land surface, as well as the recycling of water (precipitation–land surface evaporation).

In this study, SWIs and ^{3}H concentrations in rainwater, surface water and subsurface water (or shallow groundwater) were analysed to evaluate the origin of shallow groundwater in small wetlands of the CSSWs. Integration with atmospheric water budget analysis and investigation of variability in rainwater SWIs indicated that the shallow groundwater is very likely to be recharged by surface water originating from local rainfall, which is temporarily pooled in small wetlands.

Climate variations like droughts and floods have major impacts on agriculture and, because a large proportion of the population in the Cuvelai Basin lives in rural areas, drought usually has devastating effects on agricultural productivity (Christelis and Struckmeier 2001, Mendelsohn *et al* 2013). Conserving surface and subsurface waters is critical for introducing FDACS to CSSWs. We therefore highly recommend that subsurface water be used sustainability and not be pumped intensively in the future.

5. Conclusions

This study evaluated the origin of rainwater and subsurface waters in small wetlands of the CSSWs of north-central Namibia. SWIs of HDO and $H_2{}^{18}O$ in rainwater, surface water and subsurface water (or shallow groundwater) were analysed; ^{3}H counting confirmed the SWI analyses. The rainwater samples were taken from all rainfall events in the rainy season from October 2013 to April 2014 to investigate its origin and seasonal variability. The δD and $\delta^{18}O$ in each rainwater sample were also used to the WMVs of δD and $\delta^{18}O$ in precipitation. The WMVs were calculated as ($\delta^{18}O$, δD) = (−7.4, −47.2) from 29 rainfall samples and were shown to be useful for determining how subsurface waters originated in the region.

Additionally, the atmospheric water budget was also analysed. Using TRMM 3B42 version 7 data and the ERA-Interim reanalysis data, the analyses elucidated the origins of rainwater and the variations of the isotopic ratios. We found that around three-fourths of rainwater was derived from locally to regionally recycled water. Satellite-observed OLR and complementary data from MODIS and AMSR series implied that the isotopic ratios in rainwater were affected by the evaporation of raindrops falling from convective clouds. These integrated analyses revealed that shallow groundwater in small wetlands of the CSSWs is very likely to be recharged by surface water, which is sourced from local rainfall and temporarily pooled in

the lowest part of small wetlands. This was also supported by the ^{3}H concentrations of the current rain- and subsurface waters in the region. We recommend that subsurface water should not be pumped intensively, to conserve surface and subsurface waters to introduce FDACS to CSSWs.

Acknowledgments

This study was supported by the Science and Technology Research Partnership for Sustainable Development (SATREPS) of the Japan Science and Technology Agency (JST) and the Japan International Cooperation Agency (JICA). We thank all members of the Faculty of Agriculture and Natural Resources of UNAM for their support during our field survey.

References

Christelis G and Struckmeier W 2001 *Groundwater in Namibia: An Explanation to the Hydrogeological Map* (Republic of Namibia: Ministry of Agriculture, Water and Rural Development; Ministry of Mines and Energy) p 128

Craig H 1961 Isotopic variations in meteoric waters *Science* **133** 1702–3

Dee D P *et al* 2011 The ERA-Interim reanalysis: configuration and performance of the data assimilation system *Q. J. R. Meteorol. Soc.* **137** 553–97

Gat J and Matsui E 1991 Atmospheric water balance in the Amazon Basin: An isotopic evapotranspiration model *J. Geophys. Res* **96** 13179–88

Henderson-Sellers A, Mcguffie K, Noone D and Irannejad P 2004 Using stable isotopes to evaluate basin-scale simulations of surface water budgets *J. Hydrometeor.* **5** 805–22

Hiyama T, Asai K, Kolesnikov A B, Gagarin L A and Shepelev V V 2013 Estimation of the residence time of permafrost groundwater in the middle of the Lena River basin, eastern Siberia *Environ. Res. Lett.* **8** 035040

Hiyama T, Suzuki T, Hanamura M, Mizuochi H, Kambatuku J R, Niipele J N, Fujioka Y, Ohta T and Iijima M 2014 Evaluation of surface water dynamics for water-food security in seasonal wetlands, north-central Namibia *IAHS Publ.* **364** 380–85

Huffman G J *et al* 2007 The TRMM multisatellite precipitation analysis (TMPA): quasi-global, multiyear, combined-sensor precipitation estimates at fine scales *J. Hydromet.* **8** 38–55

Iijima M, Awala S K and Mwandemele O D 2013 Introduction of subsistence rice cropping system harmonized with the water environment and human activities in seasonal wetlands in northern Namibia *Proceedings for the International Symposium of SATREPS Rice-Mahangu Project 'Agricultural Use of Seasonal Wetland Formed in Semiarid Region of Africa' (Nagoya University, Japan, 13 July 2013)* pp 4–12

International Atomic Energy Agency 2007 *Atlas of isotope hydrology—Africa* (Vienna: IAEA Library Cataloguing in Publication Data) 120 p

Kanamori H, Yasunari T and Kuraji K 2013 Modulation of the diurnal cycle of rainfall associated with the MJO observed by a dense hourly rain gauge network at Sarawak, Borneo *J. Clim.* **26** 4858–75

Kurita N and Yamada H 2008 The role of local moisture recycling evaluated using stable isotope data from over the middle of the Tibetan Plateau during the Monsoon season *J. Hydromet.* **9** 760–75

Lee H-T 2014 Climate Algorithm Theoretical Basis Document (C-ATBD): Outgoing longwave radiation (OLR)—Daily, NOAA's Climate Data Record (CDR) program *NOAA Technical Report CDRP-ATBD-0526* 46 p

Lee H-T, Schreck C J and Knapp K R 2014 Generation of the Daily OLR Climate Data Record, *2014 EUMETSAT Meteorological Satellite Conference (Geneva, Switzerland, September 2014)* pp 22–26

Mendelsohn J, Obeid el S and Roberts C 2000 *A Profile of North-central Namibia* (Windhoek, Namibia: Gamsberg Macmillan Publishers) 79 p

Mendelsohn J, Jarvis A, Roberts C and Robertson T 2002 *Atlas of Namibia—A Portrait of the Land and Its People* (The Ministry of Environment and Tourism of Namibia, David Philip Publishers) 200 p

Mendelsohn J, Jarvis A and Robertson T 2013 A profile and atlas of the Cuvelai—Etosha basin (RAISON & Gondwana Collection) 170 p

Merlivat L and Jouzel J 1979 Global climatic interpretation of the deuterium-oxygen 18 relationship for precipitation *J. Geophys. Res.* **84** 5029–33

Mizuochi H, Hiyama T, Ohta T and Nasahara K N 2014 Evaluation of the surface water distribution in north-central Namibia based on MODIS and AMSR series *Remote Sens.* **6** 7660–82

Njunge J T 2013 Natural vegetation and potential agroforestry use of the seasonal wetlands in North, Central Namibia *Proceedings for the International Symposium of SATREPS Rice-Mahangu Project 'Agricultural Use of Seasonal Wetland Formed in Semiarid Region of Africa' (Nagoya University, Japan, 13 July 2013)* pp 21–9

Peixoto J P and Oort A H 1983 The atmospheric branch of the hydrological cycle and climate *Variations in the Global Water Budget* ed A Street-Perrott, M Beran and R Ratcliffe (Dordrecht: Reidel) pp 5–65

Peixoto J P and Oort A H 1992 *Physics of Climate* (New York: AIP)

Suzuki T, Ohta T, Hiyama T, Izumi Y, Mwandemele O and Iijima M 2014 Effects of the introduction of rice on evapotranspiration in seasonal wetlands *Hydrol. Proc.* **28** 4780–94

The World Bank 2012 *World Development Indicators 2012* (Washington, DC: The World Bank) 430 p

United Nations Development Programme 2007 *Human Development Report 2007/2008. Fighting Climate Change: Human Solidarity in a Divided World* (New York: Palgrave Macmillan) 384 p

Xu H 2006 Modification of normalised difference water index (NDWI) to enhance open water features in remotely sensed imagery *Int. J. Remote Sens.* **27** 3025–33